

Is NP Aqr a new near-contact binary?[☆]

C. İbanoğlu^a, Ö. Çakırlı^{*,a}, A. Dervişoğlu^a

^aEge University, Science Faculty, Department of Astronomy and Space Sciences, 35100 Bornova, İzmir, Turkey

Abstract

We present radial velocities of the double-lined spectroscopic binary NP Aqr. The radial velocities and the optical light curves obtained by Hipparcos and ASAS-3 are analyzed separately. The masses of the primary and secondary components have been found to be 1.65 ± 0.09 and $0.99 \pm 0.05 M_{\odot}$, respectively. The cross-correlation functions indicate triple peaks which show presence of a tertiary star. The spectroscopic properties of this additional component resemble to that of the primary star. The analysis of the light curves yielded that the more massive primary star fills its corresponding Roche lobe. The secondary component is at or near Roche lobe indicating a new β Lyrae-type near-contact binary. The orbital inclination is about 40° and, therefore, the observed light variations are produced only by the proximity effects. Due to the absence of eclipses, the effective temperature of the secondary star and the radii of the components could not be determined accurately. We conclude that NP Aqr is a non-eclipsing double-lined spectroscopic binary with a distance of about 134 ± 7 pc. The absolute parameters of the components are also compared with the evolutionary models. While the location of the primary star seems to be suitable with respect to its mass in the Hertzsprung-Russell diagram, the secondary component is located as if a star having a mass less than $0.6 M_{\odot}$. This discrepancy is originated from very low effective temperature determined only from the light curve produced by proximity effects. The distance to the third star appears to be very close to that of the close binary which indicates that it may be dynamically bounded to the binary.

Key words: binaries: stars: close - binaries: eclipsing-binaries: general - binaries: spectroscopic - stars: individual: NP Aqr

1. Introduction

The light variability of NP Aquarii (=HD 198528=HIP 102935=NSV 25363) was first suspected by Tobin, Viton & Sivan (1994) during the Spacelab-1 Very Wide Field survey of UV-excess objects. This survey has revealed a variety of stellar objects with strong ultraviolet excess (see, for example, Viton et al. 1988). Perryman et al. (1997) confirmed its light variation using the H_p magnitudes obtained by the Hipparcos mission. The type of the light variability could not be classified with the available data. Later on, Otero (2003) gave the epoch of minimum

[☆]Based on observations collected at Catania Astrophysical Observatory (Italy)

*Corresponding author

Email address: omur.cakirli@ege.edu.tr (C. İbanoğlu)

8 light, the orbital period and the variability class using the ASAS-3 (Pojmanski, 2002) and Hip-
9 parcos databases. He classified the star as a β Lyrae-type eclipsing binary with an orbital period
10 of 0.806982 day and with very shallow eclipses, namely 0.1 mag. Very recently, Kazarovets
11 et al. (2006) designated the star HD 198528 as NP Aqr using the criteria of *General Catalog*
12 *of Variable Stars* in the 78th Name-list of Variable Stars. van Leeuwen (2007) re-examined the
13 Hipparcos data and concluded that NP Aqr is an eclipsing binary with a spectral type of F0V
14 at a distance of 186 ± 27 pc. He also gives wide-band B-V and V-I color indices and interstel-
15 lar reddening, E(B-V). Due to its very limited light variations and a spectral type of F0
16 Handler (1999) included the star in the γ Doradus candidates but with doubts that it may also be classified
17 as a δ Scuti type variable. Handler and Shobbrook (2002) made Johnson B, V and Cousins I_c
18 observations of the known and candidate γ Dor stars to assess the relationship between the γ Dor
19 and δ Sct stars. They found slow variations with amplitudes of several hundredths of a magnitude.
20 Taking into account a double-wave light curve they have excluded W UMa-type variability and
21 suggested a possibility of an ellipsoidal variable with a period of about 0.807 day.

22 In this paper, we use the optical spectra of NP Aqr to reveal the nature of its light variability
23 and physical properties combining with the photometric data obtained by Hipparcos and ASAS-
24 3. The paper is organized as follows. In §2 the spectroscopic observations and data analysis are
25 described. The spectroscopic and photometric results are combined and the absolute parameters
26 of the stars are derived and the structure of NP Aqr is discussed in §3. A brief conclusion is given
27 in §4.

28 **2. Spectroscopic observations**

29 Spectroscopic observations have been performed with the échelle spectrograph (FRESCO) at
30 the 91-cm telescope of Catania Astrophysical Observatory. The spectrograph is fed by the tele-
31 scope through an optical fibre (*UV-NIR*, 100 μ m core diameter) and is located, in a stable posi-
32 tion, in the room below the dome level. Spectra were recorded on a CCD camera equipped with
33 a thinned back-illuminated SiTe CCD of 1k \times 1k pixels (size 24 \times 24 μ m). The cross-dispersed
34 échelle configuration yields a resolution of about 22 000, as deduced from the full width at half
35 maximum (FWHM) of the lines of the Th-Ar calibration lamp. The spectra cover the wave-
36 length range from 4300 to 6700 Å, split into 19 orders. In this spectral region, and in particular
37 in the visual portion of the spectrum, there are several lines useful for the measurement of radial
38 velocity, as well as for spectral classification of the stars.

39 The data reduction was performed by using the échelle task of IRAF package following the
40 standard steps: background subtraction, division by a flat field spectrum given by a halogen
41 lamp, wavelength calibration using the emission lines of a Th-Ar lamp, and normalization to the
42 continuum through a polynomial fit.

43 Sixteen spectra of NP Aqr were collected during the 20 observing nights between August 2nd
44 and September 23th, 2006. Typical exposure times for the NP Aqr spectroscopic observations
45 were between 2600 and 3000 s. The signal-to-noise ratios (S/N) achieved were between 70 and
46 115, depending on atmospheric condition.

47 We also observed the radial and rotational velocity standards α Lyr (A0V), ι Psc (F7V), and
48 50 Ser (F0V) with the same instrumentation. The average S/N at continuum in the spectral
49 region of interest was 150–200 for the standard stars. Cross-correlating the spectra of NP Aqr
50 with standard stars usually yielded robust correlation peaks with a FWHM of approximately 0.18
51 Å. Fitting a Gaussian profile to these peaks allowed the center to be determined to an accuracy
52 of about 0.02 Å. This transforms to a radial velocity accuracy of ~ 1 km s⁻¹.

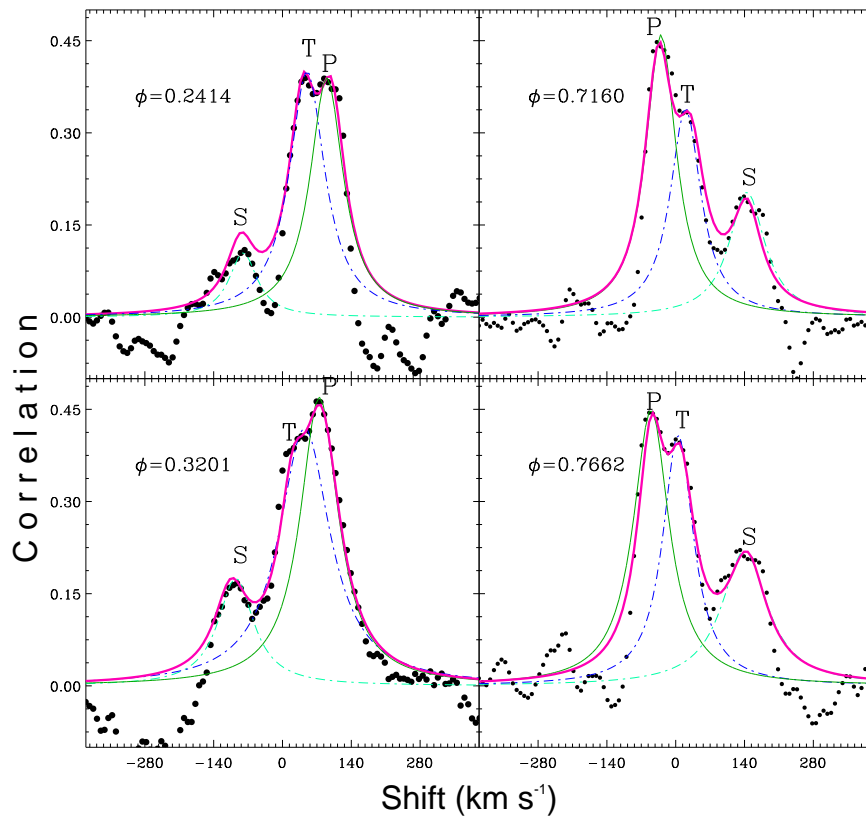


Figure 1: Sample of Cross Correlation Functions between NP Aqr and the radial velocity template spectrum (50 Ser) in various orbital phases, especially at the maxima. The orbital phases given in each panel are computed with the ephemerides given by Otero (2003). The horizontal axis is relative radial velocities, and vertical axis is normalized cross-correlation amplitude. Note that splittings at stronger peaks. P, S and T refer to the primary, secondary and tertiary stars, respectively.

Table 1: Radial velocities of the components of NP Aqr. The columns give the heliocentric Julian date, the orbital phase, the radial velocities of the two components and third star with the corresponding errors, and the average S/N of the spectrum.

HJD	Phase	Star 1		Star 2		Star 3		< S/N >
2 453 000+		V_p	σ	V_s	σ	V_t	σ	
53953.3919	0.1410	80.0	5.0	-81.0	8.1	12.6	9.8	75
53953.5325	0.3152	91.6	3.0	-94.4	8.4	26.4	8.8	88
53954.3766	0.3612	79.0	3.1	-70.9	8.5	23.5	10.0	90
53955.3771	0.6011	-27.9	5.0	103.4	14.5	35.1	11.0	87
53955.5104	0.7662	-54.0	6.7	143.6	9.2	17.3	8.8	111 ^a
53958.3998	0.3467	84.0	7.4	-83.5	8.8	25.8	6.7	95 ^a
53970.4195	0.2414	96.0	5.2	-106.4	6.8	27.6	7.1	106 ^a
53971.4214	0.4830	27.4	8.3	—	—	—	—	80
53973.3696	0.8971	-22.0	8.0	99.2	13.5	13.3	11.0	97
53975.3249	0.3201	91.6	2.4	-90.0	7.8	38.4	7.9	115 ^a
53980.3008	0.4862	25.0	7.1	—	—	—	—	75
53981.2932	0.7160	-56.4	5.6	148.1	7.7	13.9	8.0	106 ^a
53982.3099	0.9759	10.0	7.5	39.4	6.0	—	—	60
53983.2941	0.1955	93.3	5.9	-99.5	9.1	26.4	9.9	81 ^a
53985.2766	0.6522	-42.2	4.9	126.1	9.2	33.4	6.7	110 ^a

^a Used also for rotational velocity ($v \sin i$) measurements.

53 Double-lined spectroscopic binaries are characterized by the presence of two stellar spec-
54 tra that appears in the cross-correlation function (CCF) as two peaks displacing back and forth
55 according to the orbital motion of the system's components. The location of the two peaks
56 allows the measurement of the radial velocity of each component at the phase of observation.
57 The cross-correlation technique applied to digitized spectra is now one of the standard tools for
58 the measurement of radial velocities in close binary systems. This helps to explore the binary
59 mass-ratio distribution, especially in the low-mass regime.

60 The radial velocity measurements of NP Aqr were obtained by cross-correlation of each
61 échelle order of NP Aqr spectra with the spectra of the bright radial velocity standard stars α
62 Lyr (A0V), 59 Her (A3IV), ι Psc (F7V), and 50 Ser (F0V) whose radial velocities are -13.5
63 km s^{-1} , -12.4 km s^{-1} , $+5.4 \text{ km s}^{-1}$, and -45.5 km s^{-1} respectively, determined by Nordström et
64 al. (2004). For this purpose the IRAF task fxcor was used.

65 We applied the cross-correlation technique to several wavelength regions with well-defined
66 absorption lines of the primary and secondary components. These regions include the following
67 lines: Si III 4568 Å, Mg II 4481 Å, He I 5016 Å, He I 4917 Å. The stronger CCF peak shows
68 two peaks having nearly equal intensity and width, especially at both quadratures. One of these
69 stronger CCF peaks should correspond to the more massive component that also has a larger
70 contribution to the observed spectrum. To better evaluate the centroids of the peaks (i.e. the radial
71 velocity difference between the target and the template), we adopted two separate Gaussian fits
72 for the case of significant peak separation. However, we adopted three separate Gaussian fits for
73 the case of small relative line shifts at near the conjunctions when spectral lines are particularly
74 blended. In most cases, the Gaussian approximation gave reasonably good fits for the central

75 parts of the CCFs.

76 Figure 1 shows examples of CCFs at various orbital phases. The two peaks, non-blended,
77 correspond to each component of NP Aqr. The stronger peak in the CCFs corresponds to the
78 more massive component, which is also the more luminous at the observational wavelengths.
79 The CCFs shown in Fig. 1 reveal presence of at least three peaks in the spectra of NP Aqr, cor-
80 responding to phases near the quadratures. However, the spectral lines of the tertiary component
81 appear to be blended with those of the primary star. The peak between the peaks of primary
82 and secondary component could be related to a possible tertiary component. It should be noted
83 that this peak can be resolved for very limited spectra taken at both quadratures. The measured
84 radial velocities for the components of close binary and for the third star are given in Table 1.
85 However, given the noise in the CCFs, we cannot exclude the possibility that this feature is a
86 spurious peak. We estimate roughly the light contribution of the primary, secondary and tertiary
87 components in the region covered by the V bandpass as 0.44 ± 0.11 , 0.16 ± 0.04 and 0.40 ± 0.07 ,
88 respectively, using the FWHM of the CCFs.

89 2.1. Analysis of the radial velocities

90 The radial velocity measurements, listed in Table 1 together with their standard errors, are
91 weighted means of the individual values deduced from each order (see, e.g., Frasca et al. 2006).
92 The observational points and their error bars are displayed in Figure 2 as a function of orbital
93 phase, computed using the ephemeris given by Otero (2003),

$$94 \text{Min I} = \text{JDH } 2447985.661 + 0.806982E.$$

95 We also plot the radial velocities of the third star in Figure 2 (asterisks). Since the spectral
96 lines of the primary star and the tertiary component are blended we could measure the radial
97 velocities of the third star using the peaks of CCFs. For this reason the RVs of the third star appear
98 to vary with respect to the orbital phases of the binary. The solution of RVs of NP Aqr yields
99 the semi-amplitudes of the more massive, and less massive components as $K_1 = 76\pm 2 \text{ km s}^{-1}$ and
100 $K_2 = 127\pm 2 \text{ km s}^{-1}$, respectively; systemic velocity of $V_\gamma = 21\pm 1 \text{ km s}^{-1}$ and an eccentricity of
101 nearly zero, indicating a circular orbit.

102 2.2. Rotational velocities

103 The width of the cross-correlation profile is a good tool for the measurement of $v \sin i$ (see,
104 e.g., Queloz et al. 1998). The projected rotational velocities ($v \sin i$) of the two components
105 were obtained by measuring the FWHM of the CCF peaks in nine high-S/N spectra of NP Aqr
106 acquired at phases, where the spectral lines have the largest Doppler-shifts. In order to construct
107 a calibration curve $\text{FWHM} - v \sin i$, we have used an average spectrum of ι Psc, acquired with
108 the same instrumentation. Since the rotational velocity of ι Psc is very low but not zero ($v \sin i$
109 $\approx 11 \text{ km s}^{-1}$, e.g., Royer, Zorec & Fremat 2004 and references therein), it could be considered
110 as a useful template for A-type stars rotating faster than $v \sin i \approx 10 \text{ km s}^{-1}$. The spectrum of
111 ι Psc was synthetically broadened by convolution with rotational profiles of increasing $v \sin i$ in
112 steps of 5 km s^{-1} and the cross-correlation with the original one was performed at each step.
113 The FWHM of the CCF peak was measured and the $\text{FWHM} - v \sin i$ calibration was established.
114 The $v \sin i$ values of the two components of NP Aqr were derived from the FWHM of their CCF
115 peak and the aforementioned calibration relations. The FWHM values were derived for a few
116 wavelength regions and for the best spectra obtained near the quadratures. The mean projected
117 rotational velocities of the primary, secondary and tertiary components are found to be $72\pm 7 \text{ km}$
118 s^{-1} , $63\pm 10 \text{ km s}^{-1}$ and $74\pm 11 \text{ km s}^{-1}$, respectively.

119 *2.3. Spectral classification*

120 We have used our spectra to classify the primary component of NP Aqr. For this purpose we
121 have degraded the spectral resolution from 20 000 to 3 000, by convolving them with a Gaus-
122 sian kernel of the appropriate width, and we have measured the equivalent width (EW) of pho-
123 tospheric absorption lines useful for the spectral classification. We have followed the proce-
124 dures of Hernández et al. (2004), choosing hydrogen and helium lines in the blue-wavelength
125 region, where the contribution of the secondary component to the observed spectrum is neg-
126 ligible. From several spectra we measured $EW_{H\gamma} = 11.3 \pm 0.9 \text{ \AA}$, $EW_{H\alpha} = 9.79 \pm 0.11 \text{ \AA}$,
127 $EW_{H\beta} = 10.79 \pm 0.13 \text{ \AA}$, and $EW_{MgII\lambda 4481} = 0.35 \pm 0.04 \text{ \AA}$.

128 From the calibration relations EW -Spectral-type of Hernández et al. (2004), we have derived
129 a spectral type F1V with an uncertainty of about 1 spectral subclass. The effective temperature
130 deduced from the calibrations of Drilling & Landolt (2000) or de Jager & Nieuwenhuijzen (1987)
131 is about 6 900 K (F2V). The spectral-type uncertainty leads to a temperature error of $\Delta T_{\text{eff}} \approx$
132 400 K.

133 The B-V and V-I colors and the reddening in B-V are given by van Leeuwen (2007) as
134 0.348 ± 0.015 , and 0.410 ± 0.020 and 0.015 mag, respectively. Using the color-temperature rela-
135 tion given by Drilling & Landolt (2000) we estimate an effective temperature of $7\,100 \pm 90$ K for
136 the primary component of NP Aqr. However, we find $6\,850 \pm 80$ K, $7\,000 \pm 100$ K, $7\,060 \pm 100$ K
137 for the same colors using the calibrations given by Popper (1980), Alonso, Arribas & Martínez-
138 Roger (1996) and Flower (1996), respectively. On the other hand, the y/V , $b - y$, m_1 , c_1 , and β
139 values are given by Tobin, Viton & Sivan (1994) and Hauck & Mermillod (1998) as 7.640 ± 0.034 ,
140 0.201 ± 0.006 , 0.166 ± 0.006 , 0.800 ± 0.003 and 2.775 , respectively. The calibration of Drilling and
141 Landolt (2000) yields an effective temperature of $7\,170 \pm 55$ K. However, the infrared colors given
142 by Cutri et al. (2003) are $J-H=0.130 \pm 0.040$ and $H-K=0.088 \pm 0.039$ mag which correspond to a
143 temperature of $7\,100 \pm 100$ K according to the calibrations of Tokunaga (2000). The temperature
144 uncertainty of the primary component results from considerations of spectral type uncertainties
145 and temperature calibration differences. The weighted mean of the effective temperature of the
146 primary star is $7\,050 \pm 95$ K.

147 *2.4. Orbital solution*

148 The first photometric observations of NP Aqr were made by the Hipparcos mission and 49
149 H_p magnitudes were listed by van Leeuwen (2007). These magnitudes were obtained in a time
150 interval of about three years. The accuracy of the Hipparcos data is about $\sigma_{H_p} \sim 0.01$. The
151 peak-to-peak amplitude of the light variation is about 0.1 mag. These measurements are plotted
152 against the orbital phase in the bottom panel of Fig. 3.

153 NP Aqr was identified in the All-Sky Automated Survey (ASAS, Pojmanski 2004) as a de-
154 tached eclipsing binary system with a maximum, out-of-eclipse V -bandpass magnitude of 7.59^m
155 and a period of 0.8070 day. The light curve seems to exhibit periodic eclipses with depths of
156 primary and secondary eclipse of $\sim 0^m.1$ and $\sim 0^m.5$, respectively. The scatter of the data in the
157 out-of-eclipse phases was about $0^m.03$. We plot the ASAS data in the top panel of Fig. 3. It
158 is clear that both light curves are very similar but the Hipparcos magnitudes are smaller about
159 0.2 mag than those of the ASAS. Since the number of the individual observations obtained by
160 Hipparcos mission and by ASAS are not too much, we use all of them for the analysis of the light
161 curves, separately. We used the last version of the Wilson-Devinney code (Wilson and Devin-
162 ney 1971) in order to obtain the inclination of the orbit, the fractional radii and luminosities of
163 the components as well as the effective temperature of the cooler component. In the light curve

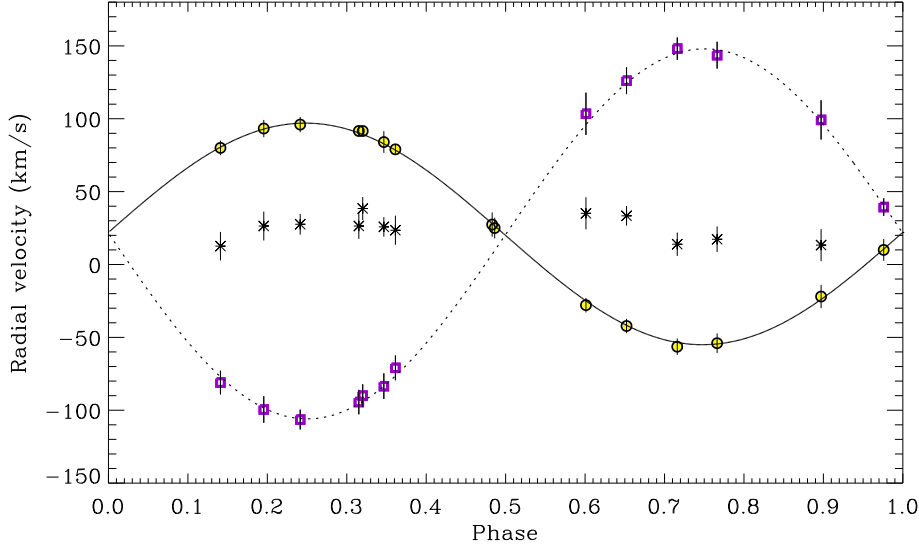


Figure 2: The observed radial velocities of NP Aqr as a function of orbital phase, with the velocity curves corresponding to the adopted orbital elements drawn through them. Open circles and squares represent the velocities of the primary and secondary components, respectively, and the asterisks represent the velocities of the tertiary component. The vertical lines on the velocities indicate their error bars.

164 solution we keep some parameters fixed whose values can be estimated from radial velocities
 165 and global stellar properties. The limb-darkening coefficients were estimated from van Hamme
 166 (1993), the gravity-darkening exponents were assumed to be $g_1=1.0$ and $g_2=0.32$, according
 167 to the von Zeipel's law, because the secondary component seems to have convective envelope.
 168 The bolometric albedos were set to $A_1=1.0$ and $A_2=0.5$ (Lucy 1967), suitable for the radiative
 169 and convective envelopes. The mass ratio, the key parameter in the solution, is taken to be 0.6
 170 adopted from the radial velocity analysis.

171 We started the light curve analysis with effective temperature of 7050 K for the primary
 172 component. Initially, the Mode-2 of the Wilson-Devinney code, referring to the detached Algols,
 173 was adopted for the analysis of the light curves. The adjustable parameters in the analysis were
 174 the inclination of the orbit (i), the surface potentials (Ω_1, Ω_2), and the effective temperature of
 175 the secondary (T_2), the luminosity of the primary star (L_1) and light contribution of the tertiary
 176 component (l_3). Using trial-and-error method we could not obtain a set of parameters, which
 177 marginally represented the observed light curves. So, we kept the orbital inclination as fixed,
 178 starting from 38 to 45 degrees. The iterations were carried out automatically until convergence,
 179 and a solution was defined as the set of parameters for which the differential corrections were
 180 smaller than the probable errors. However, after a few runs we found that the primary star's
 181 volume exceeded its inner Roche lobe whereas the secondary star was inside its lobe. So, we
 182 arrived at a decision that NP Aqr is not a detached system. Next, we tried *Mode-3* (for contact
 183 systems), *Mode-4* (primary star fills its lobe) and *Mode-5* (secondary star fills its lobe). The fits
 184 of the computed light curves obtained with Mode-4 to the observations at an inclination of 40°
 185 are satisfactory. The smallest sum of residuals squared was also arrived at an inclination of 40° .

186 Since spectroscopic observations revealed signs of a tertiary component which contributes an
187 amount of light as large as the primary component we also took the value of (l_3) as an adjustable
188 parameter. The value of l_3 in units of total triple star system light was estimated to be 0.08, too
189 small compared with the estimate from spectra. If we increase the inclination of the orbit to 41°
190 the eclipses set in and the light contribution of the third star can be better determined. When
191 the orbital inclination of the binary is taken as 44° the light contribution of the third star reaches
192 to 0.20, almost half of the value obtained from the spectra. However, photometric light curves
193 obtained by Hipparcos and ASAS do not clearly show evidence of the eclipses. So, we conclude
194 that the observed low-amplitude light variations are produced by the proximity effects rather
195 than eclipses. Such a low-amplitude light variation may give unreliable solutions. Therefore, the
196 rough values of the orbital parameters were estimated in this study, whereas determination of the
197 l_3 from the available light curves appears to almost impossible.

198 The final orbital and stellar parameters from the simultaneous light curve analysis are listed
199 in Table 3. The parameters that were adjusted have standard errors as computed by the pro-
200 gram. The computed light curve is compared with the observations in Fig. 3. Since only the
201 light variations originated from the proximity effects could be observed, the real errors of the
202 parameters should be larger than those computed by the WD code. Furthermore, it should also
203 be noted that the presence of a tertiary component slightly affects the fractional luminosities of
204 the components.

205 The results of the light curve analysis indicate that NP Aqr is very similar to that so-called
206 inverse Algols. While the primary star appears to filling its Roche lobe the secondary star is very
207 close its lobe, indicating a near contact binary (NCB). This is the case for most NCBs whose
208 light curves are of the β -Lyrae type. NCBs are distinct from the contact binaries with no large-
209 scale energy transport from one component to the other. Shaw (1994) divided the NCBs into
210 two sub-groups designated by the so-called prototypes FO Vir and V1010 Oph. The stars belong
211 to the latter subclass, i.e. V1010 Oph-type NCBs, are defined as those with a normal primary
212 at or near the Roche lobe and a secondary that is up to 1.5 times oversized, but well inside the
213 Roche lobe. In Figure 4 we show the volumes of the components and their corresponding Roche
214 lobes. While the more massive primary star is filling its Roche lobe the secondary is close to
215 its lobe. Recently, Oh (2005) collected physical parameters of all the NCBs. He proposed a
216 relationship between the mass ratio and luminosity ratio of the NCBs as $(L_2/L_1)=(M_2/M_1)^{1.45}$.
217 We estimate that the secondary star has a radius of 1.67 times larger with respect to its mass. The
218 light ratio determined from the spectra is about 0.398 which is smaller only 20 per cent than that
219 computed from the mass-to-luminosity ratios relationship. These results lead to the conclusion
220 that NP Aqr fulfills almost all properties of the V1010 Oph-type NCBs and is very similar to the
221 NCB EU Hya.

222 3. Discussion

223 Combining the parameters in Tables 2 and 3, we derived the astrophysical parameters of the
224 components and other properties in Table 4. Luminosities are computed directly from the radii
225 and effective temperatures of the components. While the light contribution of the secondary com-
226 ponent to the total light of the binary is estimated from the spectra to about 0.27, the contribution
227 is derived from the light curve analysis as low as 0.05. As we mentioned in the previous sec-
228 tion neither the temperature nor the light contribution of the secondary component are estimated
229 accurately because of the lower orbital inclination, e.g. absence of eclipses. We compared the
230 positions of the components of NP Aqr in the $\log T_{eff}-\log L/L_\odot$ diagram with the evolutionary

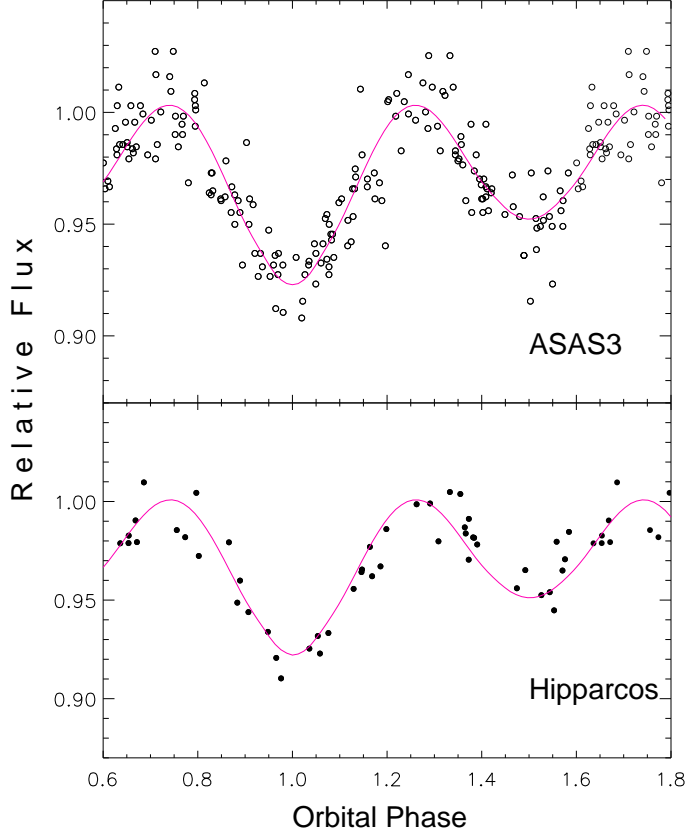


Figure 3: The light curves of NP Aqr obtained by Hipparcos (bottom panel) and ASAS-3 (top panel). The light curve corresponding to the adopted orbital elements is shown by continuous line.

Table 2: Orbital parameters for NP Aqr, obtained from the RVs analysis.

P_{orb} (days)	0.806982
V_γ (km s^{-1})	21 ± 1
K_1 (km s^{-1})	76 ± 2
K_2 (km s^{-1})	127 ± 2
$a_1 \sin i$ (R_\odot)	1.212 ± 0.032
$a_2 \sin i$ (R_\odot)	2.025 ± 0.037
q ($= M_2/M_1$)	0.598 ± 0.018
$M_1 \sin^3 i$ (M_\odot)	0.438 ± 0.018
$M_2 \sin^3 i$ (M_\odot)	0.262 ± 0.013

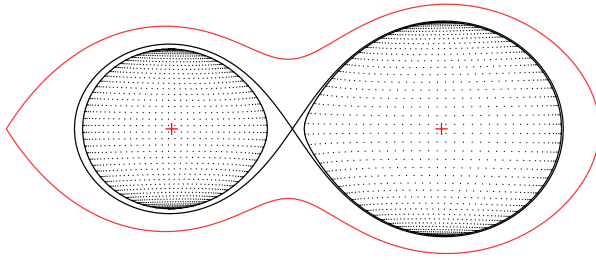


Figure 4: The three-dimensional configuration of the components of the system in the orbital plane according to our solution.

Table 3: Results of the ASAS-3 and Hipparcos light curves analysis for NP Aqr. The adopted values are the weighted means of the values determined from the individual light curves.

Parameters	ASAS3
i°	40 [Fix]
T_{eff_1} (K)	7 050[Fix]
T_{eff_2} (K)	4250±385
Ω_2	0.306±0.012
r_1	0.423±0.013
r_2	0.334±0.020
$L_1/(L_1 + L_2)$	0.95±0.04
$L_2/(L_1 + L_2)$	0.05±0.03
χ^2	0.049

Table 4: Fundamental parameters of the system.

Parameter	Primary	Secondary
Mass (M_{\odot})	1.65 ± 0.09	0.99 ± 0.05
Radius (R_{\odot})	2.13 ± 0.09	1.67 ± 0.07
$\log g$ ($cg s$)	4.00 ± 0.02	3.99 ± 0.02
T_{eff} (K)	7050 ± 95	4250 ± 385
$\log (L/L_{\odot})$	1.00 ± 0.04	-0.08 ± 0.16
$(v \sin i)_{calc.}$ ($km s^{-1}$)	86 ± 1	68 ± 2
$(v \sin i)_{obs.}$ ($km s^{-1}$)	72 ± 7	63 ± 10
d (pc)	134 ± 7	

231 tracks of Girardi et al. (2002), as shown in Fig. 5. The absolute parameters of the primary
232 star place it very close to the evolutionary track of a $1.65 M_{\odot}$ single star with solar abundance.
233 However, the secondary component appears to have lower luminosity and lower effective tem-
234 perature with respect to its mass. As we noted in the section dealing with the light curve analysis
235 the observed light variation of NP Aqr is produced only from the proximity effects. Due to the
236 lower orbital inclination eclipse phenomena are not produced. In addition, presence of a third
237 component also lightens the effect originated from the proximity of close binary. Therefore, the
238 analysis of the observed light curves can not yield the accurate parameters of the binary. We do
239 not want to make further speculation about the location of the less massive component in the HR
240 diagram and its evolutionary status, due to the very poor estimation of its parameters.

241 NP Aqr was measured by the Hipparcos mission, but the published parallax is rather uncer-
242 tain. In the first (Perryman et al. 1997) and the last (van Leeuwen 2007) versions of the Hipparcos
243 catalogs the parallaxes are given as $\pi_{Hip} = 5.50 \pm 1.31$ and 5.39 ± 0.76 mas, respectively. The latter
244 corresponds to a formal distance of 186 ± 27 pc. Based on the BVIJHK magnitudes of the binary,
245 cleaned from the contribution of third body, interstellar extinction given by Tobin, Viton & Sivan
246 (1994) and the bolometric corrections given by Girardi et al. (2002) we estimate a weighted
247 distance to the spectroscopic binary NP Aqr to be 134 ± 7 pc. The distance to the system deter-
248 mined in this study has very low uncertainty when compared with that measured by Hipparcos
249 mission. The third star has characteristics of an F1-2 main-sequence star, similar to the primary
250 component of the spectroscopic close binary, which would give it an absolute magnitude of about
251 3.2 ± 0.5 mag and a distance of about 122 ± 28 pc, if it is a single star. This result indicates that
252 the third star would plausibly be dynamically bounded to the close binary. New spectra of the
253 NP Aqr with the higher S/N ratio and resolution are needed to clarify the nature of the third star.

254 4. Conclusion

255 The first spectroscopic observations of the relatively short-period close binary NP Aqr are
256 presented. CCFs indicate that NP Aqr is a triple system. The radial velocities of both components
257 are obtained and analyzed for the spectroscopic elements. NP Aqr has been observed also by
258 the Hipparcos mission and ASAS-3 which yielded almost complete light curves of the system.
259 Both light curves are analyzed separately and the resultant orbital elements are determined. The
260 analysis of the light curves revealed that the light variation with an amount of about 0.1 mag
261 is produced from the proximity effects. In other words, NP Aqr is a double-lined, non-eclipsing
262 spectroscopic binary. The radii of the components and effective temperature of the secondary star

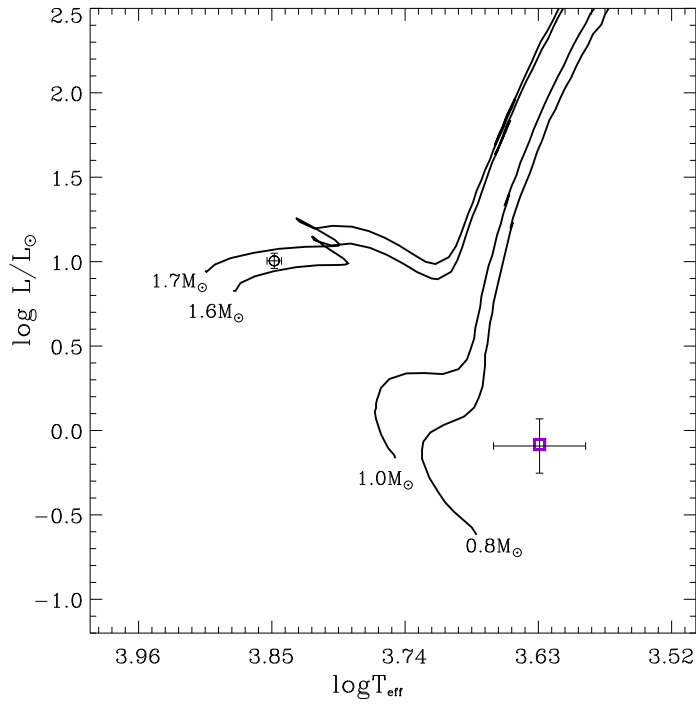


Figure 5: Comparison between evolutionary models and the physical parameters of NP Aqr in the $\log T_{\text{eff}} - \log L/L_{\odot}$ diagram. Theoretical evolutionary tracks with $Z = Z_{\odot}$ and masses of 0.8, 1.0, 1.6 and $1.7 M_{\odot}$ are adopted from Girardi et al. (2000). The circle and square denote the primary and secondary stars, respectively.

263 could be determined with great uncertainty due to the absence of the eclipses and also presence of
264 a third star. Comparing stellar evolutionary models for the mass of the components we find that
265 location of the primary star in the HR diagram is suitable with its mass. However, the secondary
266 star looks like a low-mass star. While the radius of this star is as large as 1.67 times with respect
267 to its mass, the effective temperature is unexpectedly low. The effective temperatures of the
268 binary star's components can be determined by comparing the depths of the eclipses. Since the
269 stars of NP Aqr do not show eclipses due to the small orbital inclination, the eclipses do not set
270 in. Our analysis indicates that the star NP Aqr shows most of the characteristics of the so-called
271 near-contact binaries. Moreover, we detected a third component in the system NP Aqr. The third
272 star looks like the primary component in the spectra. Using this property and assuming that it is
273 a main-sequence star we determined its distance to be 122 pc, at nearly the same distance with
274 the spectroscopic binary.

275 Acknowledgments

276 We thank Prof. G. Strazzulla, director of the Catania Astrophysical Observatory, and Dr.
277 G. Leto, responsible for the M. G. Fracastoro observing station for their warm hospitality and
278 allowance of telescope time for the observations. In addition, ÖÇ is grateful to all the people
279 working at the Catania Astrophysical Observatory for creating a stimulating and enjoyable at-
280 mosphere and, in particular, to the technical staff of the OAC, namely P. Bruno, G. Carbonaro,
281 A. Distefano, M. Miraglia, A. Micciché, and G. Occhipinti, for the valuable support in carry-
282 ing out the observations. EBİLTEM Ege University Science Foundation Project No:08/BİL/0.27
283 and Turkish Scientific and Technical Research Council for supporting this work through grant
284 Nr. 108T210. This research has been also partially supported by INAF and Italian MIUR. This
285 research has been made use of the ADS and CDS databases, operated at the CDS, Strasbourg,
286 France.

287 References

- 288 [] Alonso A., Arribas S., Martnez-Roger C., 1996, AAS, 117, 227
289 [] Cutri R. M., et al., 2003, The IRSA 2MASS All-Sky Point Source Catalog, NASA/IPAC Infrared Science
290 Archive. <http://irsa.ipac.caltech.edu/applications/Gator/>
291 [] de Jager C., Nieuwenhuijzen H., 1987, A&A, 177, 217
292 [] Drilling J. S., Landolt A. U., 2000, Allen's astrophysical quantities, 4th ed. Edited by Arthur N. Cox. ISBN: 0-387-
293 98746-0. Publisher: New York: AIP Press; Springer, 2000, p.381
294 [] Flower P. J., 1996, ApJ, 469, 355
295 [] Frasca A., Guillout P., Marilli E., Freire Ferrero R., Biazzo K., Klutsch A., 2006, A&A, 454, 301
296 [] Girardi L., Bertelli G., Bressan A., Chiosi C., Groenewegen M. A. T., Marigo P., Salasnich B., Weiss A., 2002, A&A,
297 391, 195
298 [] Handler G., 1999, MNRAS, 309, L19
299 [] Handler G., & Shobbrook R. R., 2002, MNRAS, 333, 251
300 [] Hauck B., Mermillod M., 1998, A&AS, 129, 431
301 [] Hernández J., Calvet N., Briceño C., Hartmann L., Berlind P., 2004, AJ, 127, 1682
302 [] Kazarovets E.V., Samus, N.N., Durlevich O.V., Kireeva N.N., Pastukhova E.N., 2006, IBVS, No.5721
303 [] Lucy L. B., 1967, Z. Astrophys., 65, 89
304 [] Nordström B., Mayor M., Holmberg J., Pont F., Jorgensen B. R., Olsen E. H., Udry S., Mowlavi N., 2004, A&A, 418,
305 989
306 [] Perryman M.A.C., et al., 1997, AA 323, L49
307 [] Pojmanski G., 2002, AcA, 52, 397
308 [] Popper D. M., 1980, ARA&A, 18, 115
309 [] Queloz D., Allain S., Mermillod J.-C., Bouvier J., Mayor M., 1998, A&A, 335, 183

- 310 [] Royer F., Zorec J., Fremat Y., 2004, "The A-Star Puzzle", held in Poprad, Slovakia, July 8-13, 2004. Edited by
311 J. Zverko, J. Ziznovsky, S.J. Adelman, and W.W. Weiss, IAU Symposium, No. 224. Cambridge, UK: Cambridge
312 University Press, p.109
- 313 [] Shaw J. S., 1990, in Active Close Binaries, ed. C. İbanođlu, (Dordrecht; Kluwer), 241
- 314 [] Tokunaga A. T., 2000, "Allen's astrophysical quantities", Fourth Edition, ed. A.N.Cox (Springer), p.143
- 315 [] Tobin W., Viton M. & Sivan J.-P., 1994, A&AS, 107, 385
- 316 [] Oh Kyu-D., 2005, JASS, 22, 233O
- 317 [] Otero S. A., 2003, IBVS, 5480
- 318 [] Viton M., Burgarella D., Cassatella A. & Prevot L., 1988, A&A, 205, 147
- 319 [] van Hamme W., 1993, AJ, 106, 2096
- 320 [] van Leeuwen F., 2007, A&A, 474, 653
- 321 [] Wilson R.E. and Devinney E.J., 1971, ApJ, 166, 605
- 322 [] ESA 1997, ESA SP-1200, The Hipparcos and Tycho Catalogues. ESA, Noordwijk
- 323 [] Southworth J., Smalley B., Maxted P. F. L., Claret A., Etzel P. B., 2005, MNRAS, 363, 529